Available online at www.sciencedirect.com
ScienceDirect
Progress in Biophysics and Molecular Biology 97 (2008) 217–231
Progress in Biophysics & Molecular Biology
www.elsevier.com/locate/pbiomolbio

Stretch-activated currents in cardiomyocytes isolated from rabbit pulmonary veins

Chang Ahn Seol[a], Won Tae Kim[a], Jeong Mi Ha[a], Han Choe[a], Yeon Jin Jang[a], Jae Boum Youm[b], Yung E. Earm[c], Chae Hun Leem[a,*]

[a]*Department of Physiology, University of Ulsan College of Medicine, 388-1 Poongnap-Dong Songpa-Ku, Seoul 138-736, Republic of Korea*
[b]*National Research Laboratory for Mitochondrial Signaling, Department of Physiology and Biophysics, College of Medicine, Cardiovascular and Metabolic Disease Center Inje, University, Busan 614-735, Republic of Korea*
[c]*Department of Physiology and Biophysics, Seoul National University College of Medicine, 28 Yeongeon-Dong Jongno-Gu, Seoul 110-799, Republic of Korea*

Available online 15 February 2008

Abstract

Evidence is growing of a relationship between atrial dilation and atrial fibrillation (AF), the most prevalent type of arrhythmia. Pulmonary veins, which are important ectopic foci for provoking AF, are of increasing interest in relation to the early development of AF. Here, using single cardiomyocytes isolated from rabbit pulmonary veins, we characterised the stretch-activated currents induced by swelling and axial mechanical stretching. Swelling induced both a stretch-activated nonselective cationic current (NSC) and a Cl^- current. The swelling-induced Cl^- current ($I_{Cl,swell}$) was inhibited by DIDS, whereas the swelling-induced NSC ($I_{NSC,swell}$) was inhibited by Gd^{3+}. The cationic selectivity of the $I_{NSC,swell}$ was $K^+ > Cs^+ > Na^+ > Li^+$, whilst the P_K/P_{Na}, P_{Cs}/P_{Na}, and P_{Li}/P_{Na} permeability ratios were 2.84, 1.86, and 0.85, respectively. Activation of the $I_{NSC,swell}$ was faster than that of the $I_{Cl,swell}$. Given a high K^+ concentration in the bath solution, the $I_{NSC,swell}$ showed limited amplitude (<-70 mV). Mechanical stretching induced an immediate Gd^{3+}- and streptomycin-sensitive NSC ($I_{NSC,stretch}$) that was permeable to Na^+, K^+, Cs^+ and NMDG. Persistent stretching activated a DIDS-sensitive current ($I_{Cl,stretch}$). The $I_{NSC,stretch}$, but not the $I_{NSC,swell}$, was completely blocked by 400 μM streptomycin; therefore, the two currents may not be associated with the same channel. In addition, the type of current induced may depend on the type of stretching. Thus, stretch-induced anionic and cationic currents are functionally present in the cardiomyocytes of the main pulmonary veins of rabbits, and they may have pathophysiological roles in the development of AF under stretched conditions.

Keywords: Cardiomyocytes in pulmonary veins; Hypotonic challenge; Mechanical stretch; Mechanical stretch-activated nonselective current; Swelling-induced nonselective current; Swelling-activated Cl^- current; Mechanical stretch-activated Cl^- current

*Corresponding author. Tel.: +82 2 3010 4287/+1 858 245 4763; fax: +82 2 3010 8029.
E-mail addresses: leemch@amc.seoul.kr, leemch@gmail.com (C.H. Leem).

0079-6107/$ - see front matter © 2008 Elsevier Ltd. All rights reserved.
doi:10.1016/j.pbiomolbio.2008.02.008

Contents

1. Introduction

Atrial fibrillation (AF) is the most common type of arrhythmia (Sra et al., 2000) and the most common arrhythmia-related cause of hospital admission (Bialy et al., 1992; Ruskin and Singh, 2004), and its incidence and prevalence increase with age (Wolf et al., 1991; Heeringa et al., 2006). However, the exact aetiology of AF is not fully resolved (Nattel et al., 2000; Nattel, 2002). AF is classified into three distinct categories: paroxysmal, persistent, and permanent or chronic (Levy, 1998; Sra et al., 2000). The multiple reentrant wavelet hypothesis (Moe and Abildskov, 1959) is generally accepted as the mechanism of chronic AF based on the elegant mapping studies of Allessie et al. (1982, 1985). Two independent experiments (Morillo et al., 1995; Wijffels et al., 1995) showed that tachycardia-induced electrical remodelling in the atria could develop into AF. This phenomenon was referred to as "AF begets AF" (Wijffels et al., 1995). Therefore, paroxysmal AF may develop into chronic AF by atrial remodelling, although the cause of paroxysmal AF is unknown. In fact, about 30% of cases of paroxysmal AF progress into chronic AF (Levy, 1998).

Several cardiac disorders may predispose one to AF, including coronary artery disease, pericarditis, mitral valve disease, congenital heart disease (CHD), thyrotoxic heart disease, and hypertension (Benjamin et al., 1994; Nattel, 2002). These disorders are thought to promote AF by increasing atrial pressure and/or by causing atrial dilatation (Vaziri et al., 1994; Psaty et al., 1997; Vasan et al., 1997). Experimentally induced atrial dilatation was shown to induce AF in dogs, cats, and rabbits (Boyden et al., 1982, 1984; Sideris et al., 1994; Ravelli and Allessie, 1997), although the precise mechanisms remain undefined. In a recent report, Tarantula peptide, an inhibitor of stretch-activated nonselective cationic channels (SACs), was shown to inhibit AF, suggesting that SACs may be related to the genesis of AF (Bode et al., 2001).

Haissaguerre et al. demonstrated that more than 90% of patients with paroxysmal AF had ectopic foci in their pulmonary veins (PVs) (Haissaguerre et al., 1998). The peculiar structure of the junction between the PV and left atrium, referred to as a "myocardial sleeve" (Nathan and Eliakim, 1966; Seol et al., 2007), involves an extension of the myocardium from the left atrium into the PV. In addition, the cardiomyocytes of the PV have peculiar electrical characteristics compared to atrial cardiomyocytes (Ehrlich et al., 2003). Spontaneous action potentials (SAPs) were recorded in the extrapulmonary veins of guinea pigs that could be retrogradely propagated to the atrium (Tasaki, 1969; Cheung, 1981a, b), whilst SAPs with diastolic depolarisation were observed in more than 75% of the cardiomyocytes in rabbit PVs (Nam et al., 2000; Chen et al., 2002; Seol et al., 2007). Studies of the ionic currents in dog and rabbit PV cardiomyocytes have identified several types of currents, including acetylcholine-activated K^+ currents ($I_{K,Ach}$), Na^+ currents (I_{Na}), L-type

Ca^{2+} currents (I_{CaL}), Na^{+}–Ca^{2+} exchange currents (I_{ncx}), T-type Ca^{2+} currents (I_{CaT}), inward rectifier K^{+} currents (I_{K1}), delayed rectifier K^{+} currents (I_{Ks}, I_{Kr}), hyperpolarisation-activated K^{+} currents (I_{KH}), and Ca^{2+}-activated Cl^{-} currents ($I_{Ca,Cl}$) (Choi et al., 2001; Chen et al., 2002; Ehrlich et al., 2003, 2004; Leem et al., 2006; Seol et al., 2007). Moreover, the first integrative simulation of a SAP was recently reported (Seol et al., 2007).

Kalifa et al. (2003) reported that an increase in intra-atrial pressure in sheep hearts increased the rate of wave production from the superior PV (Kalifa et al., 2003). It was also reported that the incidence and firing rate of spontaneous activity and the incidence of early afterdepolarisations (EADs) and delayed afterdepolarisations (DADs) increased in PVs after stretching, and that stretch-activated channel blockers such as gadolinium and streptomycin reduced the amount of stretch-induced spontaneous activity (Chang et al., 2007). Mechanical stretching of the cardiac cell membrane can activate stretch-activated cationic currents in ventricular or atrial cardiomyocytes (Bett and Sachs, 1997; Hu and Sachs, 1997; Cazorla et al., 1999) and stretch-activated anionic currents in rabbit ventricular myocytes (Browe and Baumgarten, 2003). Thus, stretching may increase the amount of ectopic activity in PVs by activating stretch-induced currents. In this study, we sought to identify and characterise the currents in single cardiomyocytes isolated from PVs in response to swelling and mechanical stretching.

2. Materials and methods

The protocol used to isolate single PV cardiomyocytes was described previously (Leem et al., 2006; Seol et al., 2007). Briefly, the heart and lungs of anaesthetised male New Zealand white rabbits (1.5–1.6 kg) were rapidly excised, perfused retrogradely using a Langendorff perfusion system, and digested with collagenase. Each digested heart was then dismounted from the Langendorff system and the main PV was rapidly excised from the left atrium. The junction between the PV and left atrium was easily identified by a colour change, from brown in the atrium to white in the PV. The dissected PVs were then immersed in enzyme solution at room temperature (23–25 °C) for 20 min. Individual cardiomyocytes were isolated from the PVs by gentle agitation in modified Kraftbrühe (KB) medium (Isenberg and Klockner, 1982). The cells were stored in modified KB medium at 4 °C until use. All cells were used within 8 h of isolation.

The composition of each experimental solution is listed in Table 1. Solutions I and III–VIII contained a low concentration of Cl^{-} to minimise the amplitude of the $I_{Cl,swell}$, which was large compared to the amplitudes of the other activated currents. The pH of the pipette and bath solutions was adjusted to 7.2 and 7.4, respectively, at 37 °C. Swelling was induced by a hypotonic challenge involving the removal of mannitol from the bath solution (V–IX), which had about 70% the osmolarity of the control solution. By substituting Cs^{+} with *N*-methyl-D-glucamine (NMDG) in the pipette solution and glutamate with Cl^{-} in the bath solution, we were able to identify the time course of activation for the cationic and anionic currents simultaneously. To evaluate the permeability of other monovalent cations, the Na^{+} in the bath solution was replaced by K^{+}, Cs^{+}, or Li^{+} using a Cs^{+}-based pipette solution. To block all other currents except the stretch-activated cationic currents (I_{SAC}) and $I_{Cl,swell}$, the following ion channel blockers were used: 17–40 mM TEACl (I_{to}), 1 mM $BaCl_2$ (I_{K1} and I_{KH}), 10 μM E-4031 (or 100 nM astemizole, I_{Kr}), 100 nM L-768,673 (I_{Ks}), 1 mM $CdCl_2$ (I_{Na}), and 10 μM nifedipine (I_{CaL}). Since 10 mM TEACl is sufficient to block I_{to}, the concentration of TEACl was altered to match the osmolarity of each solution. All intracellular Ca^{2+}-activated currents (I_{ncx} and $I_{Ca,Cl}$) were inhibited by the inclusion of 10 mM EGTA in the pipette solution. To block I_{NSC} and $I_{Cl,swell}$, 100 μM $GdCl_3$ or 400 μM streptomycin and 100 μM DIDS was used, respectively. All chemicals were obtained from Sigma (USA) except nifedipine (RBI, USA), E-4031 (Wako, Japan), DIDS (Calbiochem, Germany), and L-768,673 (Merck, USA).

The activation of each current was recorded using whole-cell patch clamp techniques with a holding potential of −40 mV. The pulse protocol included a step pulse to +70 mV for 100 ms, followed by a ramp pulse from +70 to −120 mV for 1 s and a step pulse to −120 mV for 100 ms; thereafter, pulses were given every 15 s. All possible junction potentials were corrected using pClamp 9.0. Images of the cells were captured every 15 s using a CCD camera (Cascade 650; Photometrics, USA) and Metamorph software (version 6.3.6; Molecular Devices Corporation, USA). Changes in cell width were analysed using Metamorph. Because the

Table 1
The composition of the experimental solutions (mM)

Ions	I[a]	II[a]	III[a]	IV[b]	V[b]	VI[b]	VII[b]	VIII[b]	IX[b]	X[b]	XI[b]
Na^+				85				85		111.5	
K^+					85				85		111.5
Cs^+	80	118				85					
Li^+							85				
Cl^-	20	125	20	26	26	26	26	106	106	155.5	155.5
$Glutamate^-$	48		105	80	80	80	80				
TEA^+	20	40	20	17	17	17	17	17	17	40	40
Mannitol	116			99	99	99	99	99	99		
Ca^{2+}				2	2	2	2	2	2	2	2
Mg^{2+}				0.5	0.5	0.5	0.5	0.5	0.5	0.5	0.5
$NMDG^+$			138								
HEPES	10	10	10	10	10	10	10	10	10	10	10
EGTA	10	10	10								
MgATP	5	5	5								
CP[c]	5	5	5								
Malate	1	1	1								
Glucose				11	11	11	11	11	11	11	11
Calculated osmolarity	330	329	329	332.5	332.5	332.5	332.5	332.5	332.5	332.5	332.5
Measured osmolarity[d]	302±2	297±2	310±3	303±1	314±2	320±2	315±2	311±4	312±2	300±3	295±1

[a]Composition of the pipette solution.
[b]Each bath solution also contained 1 mM Ba^{2+}, 1 mM Cd^{2+}, 100 nM L-768,673, 10 μM E-4031 (or 100 nM astemizole), and 10 μM nifedipine.
[c]Creatine phosphate di–tris salt.
[d]The osmolarity was measured three times and is given as the mean±S.E.M.

cell length did not change, but the cell width increased, during the hypotonic challenge, the change in area was proportional to the change in width (Suleymanian and Baumgarten, 1996; Ogura et al., 2002). Thus, the relative cell area was calculated as follows:

$$\frac{\text{cell area}_t}{\text{cell area}_c} = \frac{\text{cell width}_t}{\text{cell width}_c},$$

where t and c are the test and control conditions, respectively.

To stretch the cell membrane directly, two microelectrodes were attached to each end of a single cell as previously described (Zhang et al., 2000). One microelectrode was set to record the whole-cell current, whilst the other, which had a sealed and blunted tip, was moved by a hydraulic manipulator (Narishige, Japan) to stretch the cell longitudinally. During the stretching process, the length of each cell increased by 10–20%.

The data are expressed as the mean±S.E.M. Statistical analysis was performed using Student's t-test. A p-value less than 0.05 was considered to be statistically significant. All experiments were carried out at 36.5±0.5 °C.

3. Results

3.1. Nonselective cationic current activated by a hypotonic challenge

Hypotonic challenge has been found to activate $I_{Cl,swell}$ in cardiomyocytes (Hagiwara et al., 1992; Sorota, 1992; Tseng, 1992; Vandenberg et al., 1994) whereas DIDS has been shown to inhibit it (Sorota, 1994; Vandenberg et al., 1994). We tested whether a hypotonic challenge could activate $I_{Cl,swell}$ in cardiomyocytes isolated from PVs. When the cells were perfused with a hypotonic solution (VIII-mannitol) in addition to pipette solution II, an outward rectifying current was gradually activated (Fig. 1). We assayed the capacitance change during swelling, but found no alteration (49.7±3.7 pF in control vs. 48.8±4.3 pF during swelling, $n = 7$, $p > 0.05$). When 100 μM DIDS was added to the bath solution, the activated current was partially suppressed. The current-to-voltage (I–V) relationship of the DIDS-sensitive current showed outward

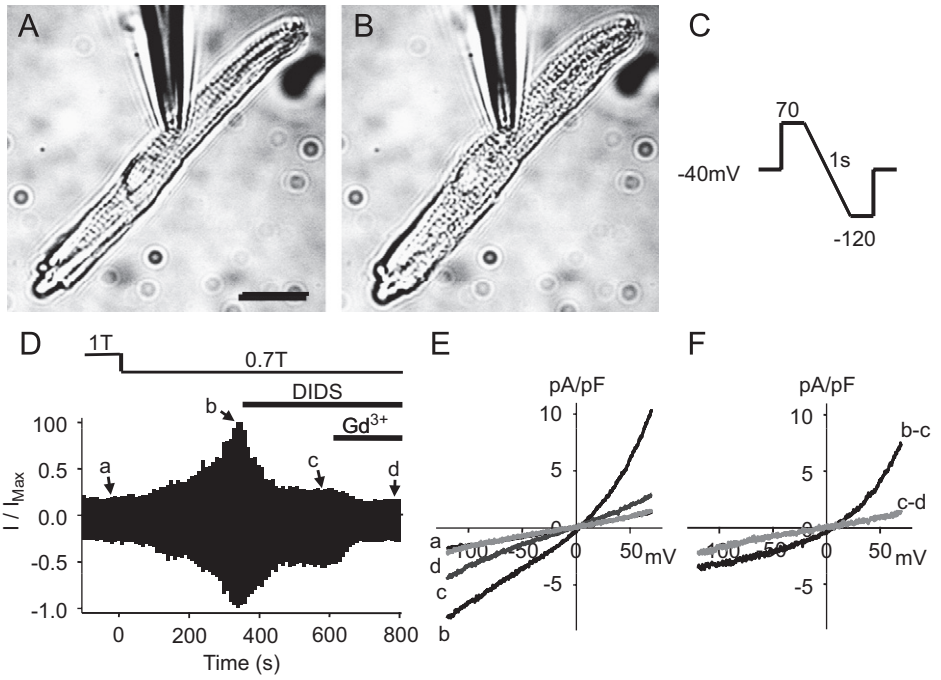

Fig. 1. The effect of DIDS and Gd^{3+} on swelling-induced stretch-activated cationic currents. Cell shape before (A) and after (B) swelling. (C) Time course analysis of the inward current amplitude at 100 mV and the outward current amplitude at +60 mV during swelling. (D) *I–V* curves in 1 T (a), 0.7 T (b), 0.7 T + 100 μM DIDS (c), and 0.7 T + 100 μM Gd^{3+} (d). (E) *I–V* curves of the subtracted currents.

rectification; however, the remaining current showed no rectification and was linear between −120 and +70 mV. Moreover, the addition of 100 μM Gd^{3+} abolished the residual activated current. The reversal potential of the DIDS-sensitive current was 1.52 ± 2.3 mV ($n = 5$), which is near the Cl^- equilibrium potential ($E_{Cl} = 4.3$ mV). The reversal potential of the Gd^{3+}-sensitive current was 1.1 ± 4.0 mV ($n = 5$). The mean amplitude of the control current prior to the hypotonic challenge was -1.7 ± 0.4 pA/pF at −100 mV ($n = 5$). The mean amplitude of the DIDS-sensitive current was -2.4 ± 0.9 pA/pF at −100 mV ($n = 5$) whilst that of the Gd^{3+}-sensitive current at −100 mV was -1.3 ± 0.2 pA/pF ($n = 5$, $p < 0.05$). Because Gd^{3+} was able to suppress the swelling-induced current, we hypothesised that the current was a nonselective cationic current and we tested this hypothesis by investigating its cationic selectivity.

3.2. Ion selectivity of the swelling-induced nonselective cationic current ($I_{NSC,\ swell}$)

To remove the $I_{Cl,swell}$, we reduced the Cl^- concentration using pipette solution I and bath solutions IV–VII (containing 100 μM DIDS). The ion selectivity of the $I_{NSC,\ swell}$ was calculated from the reversal potential in each bath solution. When Na^+ (IV) was replaced by K^+ (V), the current increased; however, the *I–V* curve showed evidence of saturation below −70 mV (Fig. 2A and B). The replacement of Na^+ (IV) by Cs^+ (VI) also increased the amplitude of the currents, but the *I–V* curve of the $I_{NSC,\ swell}$ with solution VI showed no evidence of saturation (Fig. 2C and D). The replacement of Na^+ (IV) with Li^+ (VII) increased the amplitude of the currents a little, but the reversal potential shifted to the left (Fig. 2E and F). Based on these results, the calculated permeability ratios of P_K/P_{Na}, P_{Cs}/P_{Na}, and P_{Li}/P_{Na} were 2.84 ± 0.20 ($n = 8$), 1.86 ± 0.20 ($n = 6$), and 0.85 ± 0.05 ($n = 6$), respectively. Thus, the order of ion permeability for the $I_{NSC,\ swell}$ was $K^+ > Cs^+ > Na^+ > Li^+$.

3.3. Activation of the cell membrane, $I_{NSC,\ swell}$, and $I_{Cl,swell}$ over time

To assess how the extent of stretching affects the $I_{NSC,swell}$ and $I_{Cl,swell}$ changes in the cell membrane, $I_{NSC,swell}$ and $I_{Cl,swell}$ were monitored over time. We replaced the cations in solution with NMDG and reduced

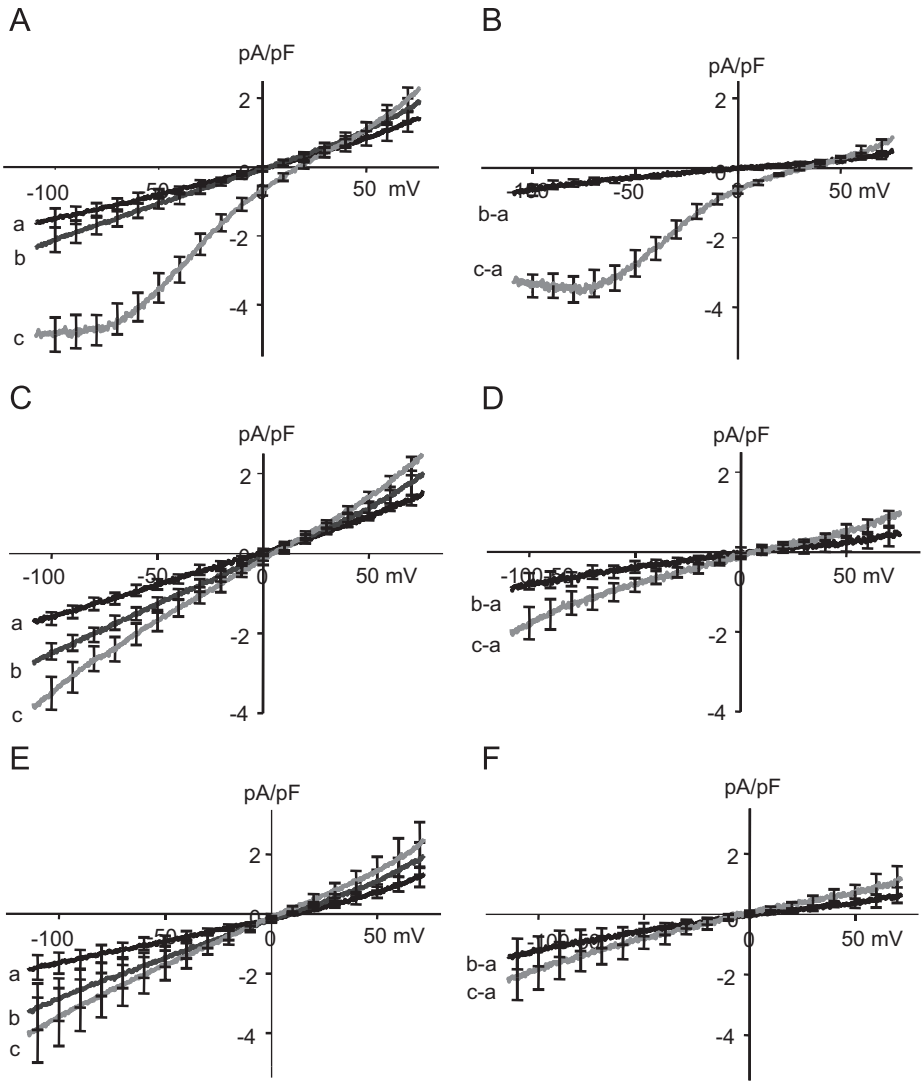

Fig. 2. The effect of substituting K^+ for Na^+ and Li^+ for Cs^+ during the hypotonic challenge. (A) *I–V* curves in 1 T (a), 0.7 T of solution IV (b), and 0.7 T of solution V (c). (C) *I– V* curves in 1 T (a), 0.7 T of solution IV (b), and 0.7 T of solution VI (c). (E) *I– V* curves in 1 T (a), 0.7 T of solution IV (b), and 0.7 T of solution VII (c). (B, D, and F) *I– V* curves of the subtracted currents. Note the inward limiting current (<-70 mV) in solution V and pipette solution I. DIDS (100 μM) was added to the bath solution with the other blockers.

the amount of Cl^- by replacing it with glutamate in the pipette solution (solution III). In addition, we used bath solution VIII. Under these conditions, the inward current at a negative voltage was mostly carried by Na^+ whilst the outward current at a positive voltage was mostly carried by Cl^-. Fig. 3A shows the effect of a hypotonic challenge on the cell membrane by whole-cell patch clamping. A 30% reduction in the osmolarity of the bath solution resulted in a $16.5 \pm 3.3\%$ ($n = 7$ at 230 s) increase in the area of the cell membrane. Fig. 3B shows the *I–V* curve at different time points after the induction of swelling, including activation of the current at $t = 1$ min. The amplitude of the outward current at $+60$ mV increased gradually; its *I–V* curve at $t = 3$ min is displayed in Fig. 3C. Similar time courses for the relative cell membrane area, inward current amplitude at -100 mV, and outward current amplitude at $+60$ mV are shown in Fig. 3D. Although the absolute amplitude of the current was larger for the outward current, the inward current was clearly activated earlier than the outward current. The reversal potential of the activated currents 3 min after the hypotonic challenge was -14.0 ± 4.3 mV ($n = 5$), which was different from the E_{Cl} value (–44 mV). These results indicate that the $I_{NSC,swell}$ was activated much sooner than the $I_{Cl,swell}$. The half-activation times of the cell area, $I_{NSC,swell}$, and

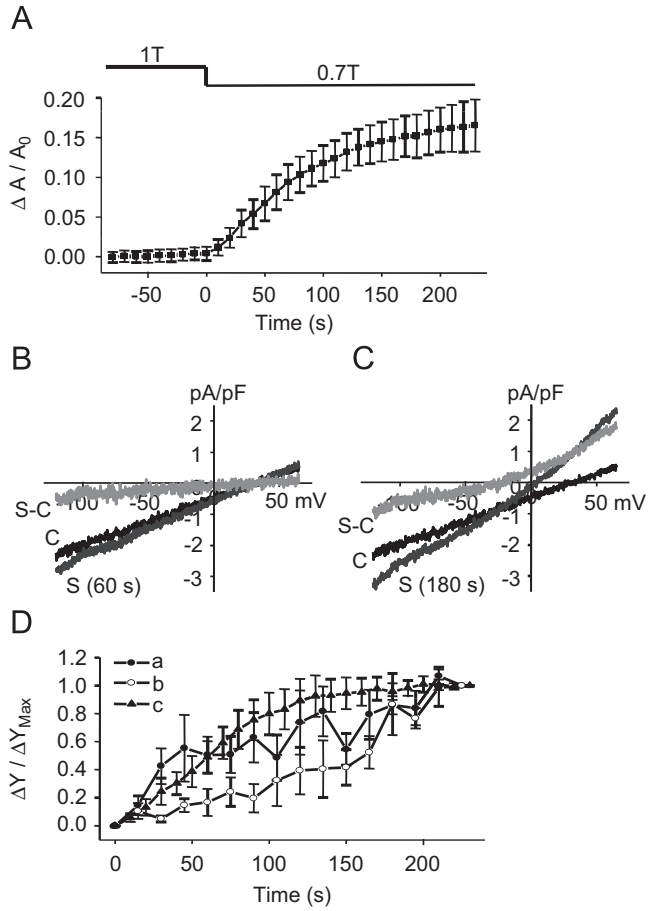

Fig. 3. Time courses of current activation by swelling. (A) The change in the relative sarcolemmal area of the clamped cells. (B) *I–V* curves of the activated currents 1 min after swelling: control (c), 1 min after swelling (s), and the subtracted current (s–c). (C) *I–V* curves of the activated currents 3 min after swelling: control (c), 3 min after swelling (s), and the subtracted current (s–c). (D) Time courses of the normalised inward current amplitude at −100 mV (a), the normalised outward current amplitude at +60 mV (b), and the relative increase in the cell membrane area (c). Pipette solution I and bath solution IV were used.

$I_{Cl,swell}$ were 68.6±8.1 s ($n = 7$), 71.2±27.5 s ($n = 5$, $p > 0.05$ for the cell area), and 146.6±22.6 s ($n = 5$, $p < 0.05$ for $I_{NSC,swell}$), respectively.

3.4. Current activation by mechanical stretching

To observe the effect of mechanical stretching, we used solutions II and X. When mechanical stretching was applied to a single cardiomyocyte, a current was abruptly activated. The stretch induced changes of the cell shape were shown in Fig. 4A and B. The mechanical stretch-induced current was easily suppressed by 100 μM $GdCl_3$ (Fig. 4C and D). The *I–V* curve of the activated currents was linear, and its reversal potential was −3.4±2.2 mV ($n = 7$).

3.5. Activation time course of the mechanical stretch-induced currents

We next conducted a time course analysis of the mechanical stretch-induced current. Using pipette solution III, the inward current was largely carried by a cation at negative voltages, whilst the outward current at positive voltages was largely carried by an anion. Mechanical stretching in solution XI abruptly activated

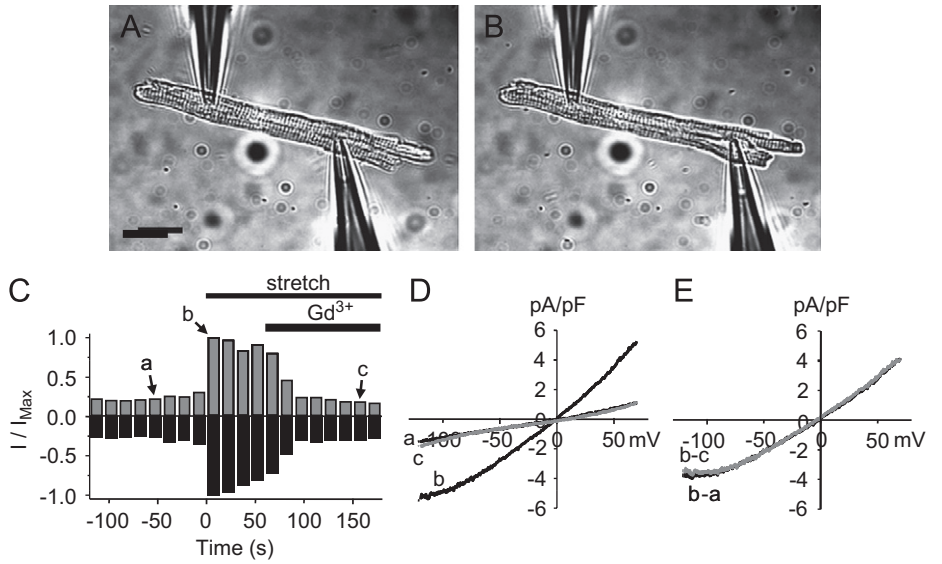

Fig. 4. Stretch-activated currents induced by axial mechanical stretching. Cell shape before (A) and after (B) stretching. (C) Time course of the inward current amplitude at −100 mV and the outward current amplitude at +60 mV during stretching. (D) *I–V* curves before stretching (a), after stretching (b), and with Gd^{3+} (c). (E) *I–V* curves of the subtracted currents. Pipette solution II and bath solution X were used.

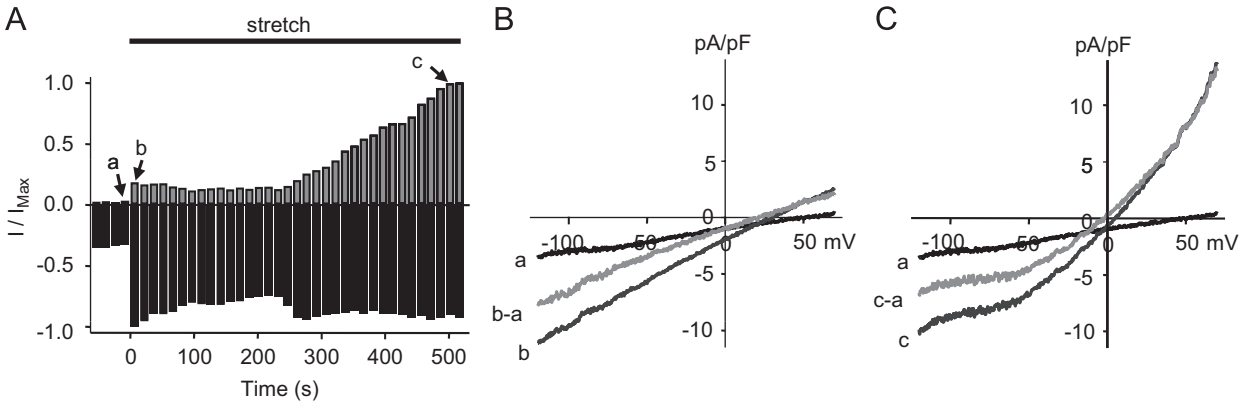

Fig. 5. Time course of the mechanical stretch-activated current. (A) Time courses of the inward current amplitude at −100 mV and the outward current amplitude at +60 mV during stretching. (B) *I–V* curves immediately after stretching: control current (a), activated current (b), and subtracted current (b–a). (C) *I–V* curves 500 s after stretching: control current (a), activated current (c), and subtracted current (c–a). Pipette solution III and bath solution XI were used.

a current with a linear *I–V* curve (Fig. 5A and B); thus, at −100 mV, the inward current must be a stretch-activated cationic current ($I_{NSC,stretch}$). Interestingly, continuous stretching gradually increased the outward current whilst the inward current remained unchanged. The change in amplitude of the current at 60 mV is shown in Fig. 5A. This current was probably carried by Cl^-; thus, it was designated a stretch-activated Cl^- current ($I_{Cl,stretch}$). The half-activation time of the $I_{Cl,stretch}$ was 350 ± 4.7 s ($n = 4$). The current amplitude (-2.7 ± 0.8 pA/pF at −100 mV, $n = 6$) using a K^+-based bath solution (XI) was larger than that (-1.6 ± 0.6 pA/pF at −100 mV, $n = 5$, $p < 0.05$) using a Na^+-based bath solution (X). The reversal potential with bath solution X was 6.5 ± 6.3 mV ($n = 5$), whilst that with solution XI was 19.9 ± 3.6 mV ($n = 6$). Based on the reversal potential, P_{Na}/P_{NMDG} was 1.8 ± 0.4 ($n = 5$) whilst P_K/P_{NMDG} was 2.8 ± 0.5 ($n = 6$).

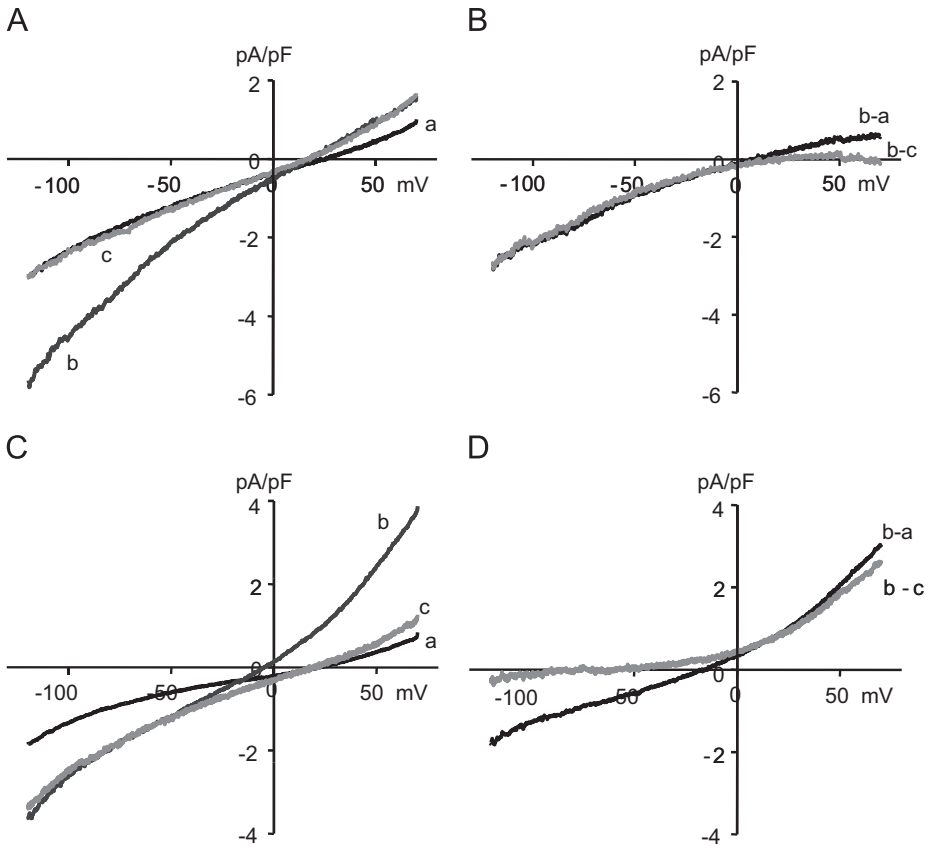

Fig. 6. Inhibition of the mechanical stretch-activated current by streptomycin and DIDS. (A) *I–V* curves: control (a), immediately after stretching in the absence of streptomycin (b), and 3 min after stretching in the presence of 400 μM streptomycin (c). (B) *I–V* curves of the subtracted currents. (C) *I–V* curves under the control condition (a), after continuous stretching for more than 7 min (b), and after 8 min of stretching in the presence of 100 μM DIDS (c). (D) *I–V* curves of the subtracted currents. Pipette solution III and bath solution X were used.

3.6. The effect of DIDS and streptomycin on the mechanical stretch-induced currents

We next tested the streptomycin and DIDS sensitivity of our mechanical stretch-activated currents using pipette solution III and bath solution X. When the cells were stretched by 10%, a current with a reversal potential of 10 mV was abruptly activated (Fig. 6A); however, the addition of 400 μM streptomycin successfully blocked the inward current, but not the outward current (b–c trace in Fig. 6B). Similar results were observed in three different cells. We also tested the effect of DIDS on the mechanically stretch-activated currents. When mechanical stretching was applied for more than 3 min, the outward current gradually increased. DIDS (100 μM) significantly inhibited the outward current and little inhibited the inward current (Fig. 6C and D); the reversal potential of the DIDS-sensitive current was -47.4 ± 2.5 mV ($n = 4$), which is near the Cl^- equilibrium potential (-54.5 mV). These results suggest that mechanical stretching activates both $I_{NSC,stretch}$ and $I_{Cl,stretch}$, and that activation of the $I_{NSC,stretch}$ occurs more rapidly than that of the $I_{Cl,stretch}$ (Fig. 7).

3.7. Differential effects of streptomycin on the $I_{NSC,swell}$ and $I_{NSC,stretch}$

We also tested the effects of streptomycin on the swelling-induced currents using a Cs^+-rich pipette solution (I) and a Na^+-based bath solution (IV). We could not use DIDS and streptomycin simultaneously because of precipitation; therefore, instead of using DIDS, we generated a low Cl^- concentration on both sides to

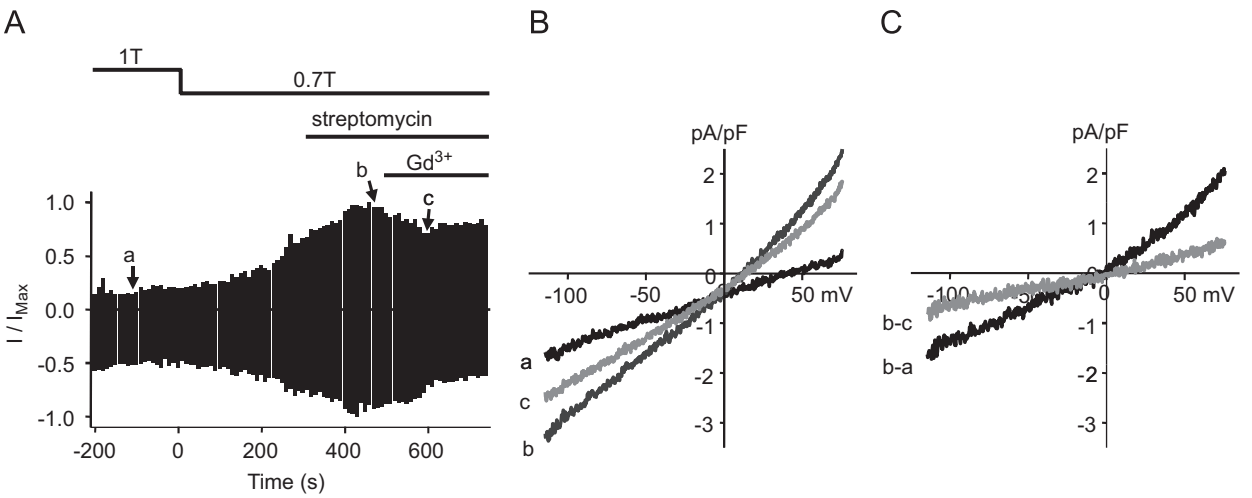

Fig. 7. Effect of streptomycin on the $I_{NSC,swell}$. (A) Time courses of the inward current amplitude at −100 mV and outward current amplitude at +60 mV during swelling. (B) *I–V* curves: control (a), just before the addition of Gd^{3+} (b), and with Gd^{3+} (c). (C) *I–V* curves of the subtracted currents.

minimise the $I_{Cl,swell}$, for which the E_{Cl} was −6.9 mV. The removal of mannitol from the bath solution activated a current with a reversal potential of -7.6 ± 2.5 mV ($n = 4$) and the addition of 400 μM streptomycin did not inhibit the swelling-activated current, which was continuously increased in the presence of 400 μM streptomycin, possibly due to the gradual activation of both the $I_{NSC,swell}$ and $I_{Cl,swell}$, with a reversal potential of -7.6 ± 2.5 mV ($n = 4$). Subsequent addition of 100 μM Gd^{3+} suppressed the activated current. The Gd^{3+}-sensitive current showed a linear *I–V* relationship, with a reversal potential of 3.2 ± 1.4 mV ($n = 4$). The reversal potential of the Gd^{3+}-insensitive activated current was -12.1 ± 2.6 mV ($n = 4$, $p < 0.05$) with a slightly outward *I–V* relationship. These results suggest that the $I_{NSC,stretch}$ and $I_{NSC,swell}$ are different entities.

4. Discussion

In this study, we measured the characteristics of the currents activated by swelling-induced stretching and axial mechanical stretching in cardiomyocytes isolated from rabbit PVs. Both types of stretching induced cationic and anionic currents, although the cationic currents were activated more quickly than the anionic currents. The activated cationic currents were nonselective regardless of the type of stretching. The $I_{NSC,swell}$, which was induced by swelling, and the $I_{NSC,stretch}$, which was induced by mechanical stretching, were both blocked by Gd^{3+}, but they had different sensitivities to streptomycin, suggesting that the currents operate through separate channels.

4.1. Swelling-activated cationic and anionic currents in PV cardiomyocytes

Why stretching of the membrane by swelling or axial mechanical stretching activated different currents is puzzling (Hu and Sachs, 1997). Cellular swelling has been reported to activate several different types of channels (Vandenberg et al., 1996), and $I_{Cl,swell}$ was reported in the hearts of several mammalian species; however, the existence of a swelling-induced cationic current in the mammalian heart has never been demonstrated. Previous studies described the effect of swelling on the K^+ channels of the mammalian heart, including I_{Ks} (Sasaki et al., 1992, 1994; Rees et al., 1995), I_{Kr} (Rees et al., 1995), and $I_{K,ATP}$ (Van Wagoner, 1993). Augmentation of the I_{CaL} by swelling was previously shown in rabbit ventricular myocytes (Matsuda et al., 1996), although it was not observed in guinea pig ventricular myocytes (Sasaki et al., 1992). In terms of nonselective cationic currents, one report described a swelling-induced nonselective cationic channel in neonatal rat atrium (Kim, 1993), whilst a second described the activation of a nonselective inward rectifying cationic current by swelling, in addition to $I_{Cl,swell}$ and its sensitivity to Gd^{3+} in freshly isolated rabbit

ventricular myocytes (Clemo and Baumgarten, 1997). Our results show the activation of an $I_{NSC,swell}$ and $I_{Cl,swell}$ in freshly isolated cardiomyocytes from rabbit PVs. Many of the characteristics of the $I_{NSC,swell}$ that we observed, including higher permeability to K^+ than Na^+, activation of the $I_{NSC,swell}$ before the $I_{Cl,swell}$, Gd^{3+} sensitivity, and Ba^{2+} insensitivity, were similar to those reported in rabbit ventricular myocytes (Clemo and Baumgarten, 1997); however, we did not observe inward rectification.

The $I_{NSC,swell}$ had a linear I–V relationship with the Cs^+-rich pipette solution when Na^+, Cs^+, or Li^+ was included in the bath solution. In contrast, when K^+ was included in the bath solution, the I–V curve showed limited amplitude below −70 mV (Fig. 2A and B). Given that very few studies have focused on whole-cell currents activated by swelling or mechanical stretching in cardiomyocytes, it was difficult to compare our results with those of other reports. In chick ventricular myocytes, the I–V curve was slightly outwardly rectified in a high-K^+ bath solution (Hu and Sachs, 1996), whilst other studies have shown a linear I–V relationship in the presence of monovalent cations on both sides (Zeng et al., 2000; Zhang et al., 2000; Kamkin et al., 2003a, b). The most similar I–V curve to ours for a stretching-activated current below −70 mV was reported in guinea pig ventricular myocytes, although the experimental conditions were different from ours (Sasaki et al., 1992). That study used a K^+-rich pipette solution and normal Tyrode bath solution without blockers and mechanical stretching. They concluded that this phenomenon might be caused by inhibition of the I_{K1} or a space problem with the clamp because of the large conductance of I_{K1}; however, they did not pursue the issue further. We previously showed (Seol et al., 2008) that the I_{K1} was extremely small in PV cardiomyocytes (1 pA/pF at −120 mV). In this study, we additionally used 1 mM Ba^{2+} and 20 mM TEA to block I_{K1}. Therefore, we are confident that we eliminated the possibility of I_{K1} activity or a space clamp problem. Several reports have demonstrated the existence of stretch-activated K^+ channels (Hu and Sachs, 1997), and the possibility exists that stretch-activated K^+ channels are responsible for limiting the current to <-70 mV. If so, the current through these stretch-activated K^+ channels should be much larger than the $I_{NSC,swell}$. Unfortunately, we were unable to find any specific blockers for stretch-activated K^+ channels; thus, we used putative K^+ channel blockers such as Ba^{2+} and TEA. Although we cannot exclude the possible involvement of stretch-activated K^+ channels, the observed effect is likely an intrinsic property of the $I_{NSC,swell}$.

The cationic selectivity we observed ($K^+ > Na^+$) was similar to that reported for the I_{NSC} in neonatal rat ventricular myocytes (Craelius, 1993), neonatal chick ventricular myocytes (Ruknudin et al., 1993; Hu and Sachs, 1996), rabbit ventricular myocytes (Clemo and Baumgarten, 1997), rat atrial myocytes ($Cs^+ > Na^+ > Li^+$) (Zhang et al., 2000), and mouse ventricular myocytes ($Cs^+ > Na^+ > Li^+ > TEA^+ > NMDG^+$) (Kamkin et al., 2003a).

4.2. Activation of cationic and anionic currents by axial mechanical stretching in PV cardiomyocytes

Several reports have shown that mechanical stretching can induce nonselective cationic currents in cardiomyocytes (Sadoshima et al., 1992; Sasaki et al., 1992; Hu and Sachs, 1996; Youm et al., 2000; Zhang et al., 2000; Kamkin et al., 2003a, b). We also observed the activation of a monovalent cation-selective current in response to axial mechanical stretching in cardiomyocytes isolated from rabbit PVs. The $I_{NSC,stretch}$, which was permeable to Cs^+, Na^+, and K^+, was activated immediately upon stretching, as shown in previous reports (Kamkin et al., 2000; Zeng et al., 2000). However, it has been suggested that mechanical stretching cannot activate Cl^--dependent currents, in contrast to swelling-induced stretching (Bett and Sachs, 1997; Hu and Sachs, 1997; Cazorla et al., 1999). In a previous report, membrane stretching induced by paramagnetic beads, which were used to stretch β1-integrins, activated both a Cl^- current and a cationic current. The characteristics of the activated Cl^- current ($I_{Cl,SAC}$) were similar to those of the $I_{Cl,swell}$ (Browe and Baumgarten, 2003) in that it was coupled to NADPH oxidase and regulated by EGF kinase via phosphatidylinositol 3-kinase and NADPH oxidase (Browe and Baumgarten, 2004, 2006). Our results also show that axial mechanical stretching can activate DIDS-sensitive, Gd^{3+}- or streptomycin-insensitive Cl^- currents in cardiomyocytes isolated from PVs. Activation of the $I_{Cl,swell}$ and $I_{Cl,stretch}$ required persistent swelling or stretching, as has been shown in other reports (Clemo and Baumgarten, 1997; Browe and Baumgarten, 2003), and the activation time course of the $I_{Cl,stretch}$ in our study was similar to that of the $I_{Cl,SAC}$ (Browe and Baumgarten, 2003). We propose that $I_{Cl,stretch}$ and $I_{Cl,swell}$ are the same current, and that it

is activated slowly because it involves a signalling cascade, as noted in a previous report (Browe and Baumgarten, 2003). Since axial mechanical stretching is very subtle and difficult to induce in a single cardiomyocyte (Hu and Sachs, 1997), we need to address whether the $I_{Cl,stretch}$ is an artefact of membrane breakage; we do not believe that it is an artefact because it was specifically blocked by DIDS. In addition, if activation of the $I_{Cl,stretch}$ was an artefact, the inward current would be expected to increase with the $I_{Cl,stretch}$ because a nonspecific leak current due to membrane breakage could not be specific to Cl^- alone; however, the inward current did not increase as the $I_{Cl,stretch}$ increased (Fig. 5A).

Interestingly, even though we replaced all of the cations in the pipette solution with NMDG, an outward current was activated at +60 mV right after stretching (Fig. 5A and B). This current was observed in the presence of DIDS (Fig. 6D), but it was successfully blocked by Gd^{3+} (data not shown). In a previous report, NMDG substitution could not abolish the mechanical stretch-activated currents in mouse ventricular myocytes (Kamkin et al., 2003a). Therefore, the outward current shown in Fig. 5A and B may have been due to NMDG permeability.

4.3. Differences between the $I_{NSC,swell}$ and $I_{NSC,stretch}$

The activation of the stretch-induced cationic currents was faster than that of the stretch-induced anionic currents, regardless of the mode of stretching. Both the $I_{NSC,swell}$ and $I_{NSC,stretch}$ were blocked by Gd^{3+}; however, the $I_{NSC,stretch}$ was suppressed by streptomycin whilst the $I_{NSC,swell}$ was not. These results suggest that PV cardiomyocytes have at least two types of stretch-induced NSCs, and that differences in channel activation may not be caused by tension differences between the modes of stretching. Incorporation of the membrane may not have occurred because the capacitances before and after swelling were similar (this may also apply to mechanical stretching under our experimental conditions). Swelling increased the membrane area by about 15%, whilst mechanical stretching increased the membrane area by about 10–20% in our experiments. If no directional differences existed in the elastic constant of the membrane, both stretches would generate the similar tension. Therefore, we suggest that the direction of the applied stretch may alter the resulting stretch-induced current. Axial stretching may activate the $I_{NSC,stretch}$ whilst the stretch induced by swelling may activate the $I_{NSC,swell}$. It would be interesting to determine the physiological roles of each mode of activation.

Interestingly, as shown in Fig. 6A and B, streptomycin blocked the inward current but had virtually no effect on the outward current. A similar voltage-dependent blocking effect was previously reported for aminoglycoside antibiotics on stretch-activated channels in chick skeletal muscles (Sokabe et al., 1993). In that study, using an inside-out patch with antibiotics in the pipette solution, antibiotics were shown to block the stretch-activated channels in a dose- and voltage-dependent manner. The half-blocking concentration of streptomycin was about 20–25 μM; thus, the 400 μM used in this study should have been sufficient to block the I_{NSC} completely. Still, we cannot exclude the possibility of variation in the sensitivity of each I_{NSC} to streptomycin.

4.4. Pathophysiological implications of stretch-activated channels in the cardiomyocytes of PVs

Atrial dilation is an independent risk factor for the development of AF (Vaziri et al., 1994; Psaty et al., 1997; Vasan et al., 1997). Atrial dilation itself may be a factor in the initiation of AF through mechanoelectric feedback (Schotten et al., 2003). The finding that a specific SAC blocker, Tarantula toxin (GsMtx-4), can block pressure-induced AF (Bode et al., 2001) is important in this respect. Since the myocardial sleeve in PVs is the extension of atrium and is much thinner than the walls of the atrium (Nathan and Eliakim, 1966; Seol et al., 2008), it may be more vulnerable to the stretching. Several reports have suggested an association between PV enlargement and AF (Lin et al., 2000; Tsao et al., 2001; Yamane et al., 2002; Knackstedt et al., 2003; Herweg et al., 2005). Experimentally, an increase in intra-atrial pressure in sheep heart increased the rate and wave production emanating from the superior pulmonary veins (Kalifa et al., 2003) and the incidence and firing rates of spontaneous activity were increased in PVs after stretch (Chang et al., 2006). Our results clearly showed the existence of the stretch activated currents in cardiac myocytes of PVs. Therefore, the development of AF may occur as follows: atrial dilation → dilation of the PVs → activation of $I_{NSC,stretch}$ → ectopic

activity in the PVs → paroxysmal AF → ionic remodelling in the atrium → chronic AF. Mechanoelectric feedback may be an essential feature of this mechanism; however, further study is required.

Acknowledgements

We thank Dr. Joseph J. Salata (MERCK) for generous gift of L-768673. We also thank Dr. Jeffrey Jacot for correcting English. This work was supported by grant no. R01-2004-000-10374-0 from the KOSEF and was supported by Korea Research Foundation Grant funded by Korea Government (MOEHRD, Basic Research Promotion Fund, KRF-2005-003-E00014).

Editor's note

Please see also related communications in this issue by Folgering et al. (2008) and Stones et al. (2008).

References

Allessie, M., Lammers, W.J.E.P., Smeets, J., Bonke, F.I.M., Hollen, J., 1982. Total mapping of atrial excitation during acetylcholine-induced atrail flutter and fibrillation in the isolated canine heart. In: Kulbertus, H.E., Olsson, S.B., Schlepper, M. (Eds.), Atrial Fibrillation. AB Hassle, MoIndal, Sweden, pp. 44–59.

Allessie, M.A., Lammers, W.J.E.P., Bonke, F.I.M., Hollen, J., 1985. Experimental evaluation of Moe's multiple wavelet hypothesis of atrial fibrillation. In: Zipes, D.P., Jalife, J. (Eds.), Cardiac Electrophysiology and Arrhythmias. Grune & Stratton, Orlando, FL, pp. 265–276.

Benjamin, E.J., Levy, D., Vaziri, S.M., D'Agostino, R.B., Belanger, A.J., Wolf, P.A., 1994. Independent risk factors for atrial fibrillation in a population-based cohort. The Framingham Heart Study. JAMA 271, 840–844.

Bett, G.C.L., Sachs, F., 1997. Cardiac mechanosensitivity and stretch-activated ion channels. Trends Cardiovasc. Med. 7, 4–8.

Bialy, D., Lehmann, H., Schumacher, D.N., 1992. Hospitalization fro arrhymia in the United States: importance of atrial fibrillation. J. Am. Coll. Cardiol. 19, 2003.

Bode, F., Sachs, F., Franz, M.R., 2001. Tarantula peptide inhibits atrial fibrillation. Nature 409, 35–36.

Boyden, P.A., Tilley, L.P., Pham, T.D., Liu, S.K., Fenoglic Jr., J.J., Wit, A.L., 1982. Effects of left atrial enlargement on atrial transmembrane potentials and structure in dogs with mitral valve fibrosis. Am. J. Cardiol. 49, 1896–1908.

Boyden, P.A., Tilley, L.P., Albala, A., Liu, S.K., Fenoglio Jr., J.J., Wit, A.L., 1984. Mechanisms for atrial arrhythmias associated with cardiomyopathy: a study of feline hearts with primary myocardial disease. Circulation 69, 1036–1047.

Browe, D.M., Baumgarten, C.M., 2003. Stretch of beta1 integrin activates an outwardly rectifying chloride current via FAK and Src in rabbit ventricular myocytes. J. Gen. Physiol. 122, 689–702.

Browe, D.M., Baumgarten, C.M., 2004. Angiotensin II (AT1) receptors and NADPH oxidase regulate Cl^- current elicited by beta1 integrin stretch in rabbit ventricular myocytes. J. Gen. Physiol. 124, 273–287.

Browe, D.M., Baumgarten, C.M., 2006. EGFR kinase regulates volume-sensitive chloride current elicited by integrin stretch via PI-3 K and NADPH oxidase in ventricular myocytes. J. Gen. Physiol. 127, 237–251.

Cazorla, O., Pascarel, C., Brette, F., Le Guennec, J.Y., 1999. Modulation of ions channels and membrane receptors activities by mechanical interventions in cardiomyocytes: possible mechanisms for mechanosensitivity. Prog. Biophys. Mol. Biol. 71, 29–58.

Chen, Y.J., Chen, S.A., Chen, Y.C., Yeh, H.I., Chang, M.S., Lin, C.I., 2002. Electrophysiology of single cardiomyocytes isolated from rabbit pulmonary veins: implication in initiation of focal atrial fibrillation. Basic. Res. Cardiol. 97, 26–34.

Chang, S.L., Chen, Y.C., Chen, Y.J., Wangcharoen, W., Lee, S.H., Lin, C.I., Chen, S.A., 2007. Mechanoelectrical feedback regulates the arrhythmogenic activity of pulmonary veins. Heart 93, 82–88.

Cheung, D.W., 1981a. Electrical activity of the pulmonary vein and its interaction with the right atrium in the guinea-pig. J. Physiol. 314, 445–456.

Cheung, D.W., 1981b. Pulmonary vein as an ectopic focus in digitalis-induced arrhythmia. Nature 294, 582–584.

Choi, K.J., Kim, W.T., Nam, G.B., Song, J.K., Kim, J.J., Park, S.W., Park, S.J., Park, C.H., Kim, Y.H., Choi, Y.S., Leem, C.H., 2001. The characteristics of spontaneous action potential of cardiac myocytes in rabbit pulmonary veins. The Korean Circulation Journal 31, 94–105.

Clemo, H.F., Baumgarten, C.M., 1997. Swelling-activated Gd^{3+}-sensitive cation current and cell volume regulation in rabbit ventricular myocytes. J. Gen. Physiol. 110, 297–312.

Craelius, W., 1993. Stretch-activation of rat cardiac myocytes. Exp. Physiol. 78, 411–423.

Ehrlich, J.R., Cha, T.J., Zhang, L., Chartier, D., Melnyk, P., Hohnloser, S.H., Nattel, S., 2003. Cellular electrophysiology of canine pulmonary vein cardiomyocytes: action potential and ionic current properties. J. Physiol. 551, 801–813.

Ehrlich, J.R., Cha, T.J., Zhang, L., Chartier, D., Villeneuve, L., Hebert, T.E., Nattel, S., 2004. Characterization of a hyperpolarization-activated time-dependent potassium current in canine cardiomyocytes from pulmonary vein myocardial sleeves and left atrium. J. Physiol. 557, 583–597.

Folgering, J.H.A., Sharif-Nacini, R., Dedman, A., Patel, A., Delmas, P., Honoré, E., 2008. Molecular basis of the mammalian pressure-sensitive ion channels: Focus on vascular mechanotransduction. Prog. Biophys. Mol. Biol. 97, 180–195.

Hagiwara, N., Masuda, H., Shoda, M., Irisawa, H., 1992. Stretch-activated anion currents of rabbit cardiac myocytes. J. Physiol. 456, 285–302.

Haissaguerre, M., Jais, P., Shah, D.C., Takahashi, A., Hocini, M., Quiniou, G., Garrigue, S., Le Mouroux, A., Le Metayer, P., Clementy, J., 1998. Spontaneous initiation of atrial fibrillation by ectopic beats originating in the pulmonary veins. N. Engl. J. Med. 339, 659–666.

Heeringa, J., van der Kuip, D.A., Hofman, A., Kors, J.A., van Herpen, G., Stricker, B.H., Stijnen, T., Lip, G.Y., Witteman, J.C., 2006. Prevalence, incidence and lifetime risk of atrial fibrillation: the Rotterdam study. Eur. Heart J. 27, 949–953.

Herweg, B., Sichrovsky, T., Polosajian, L., Rozenshtein, A., Steinberg, J.S., 2005. Hypertension and hypertensive heart disease are associated with increased ostial pulmonary vein diameter. J. Cardiovasc. Electrophysiol. 16, 2–5.

Hu, H., Sachs, F., 1996. Mechanically activated currents in chick heart cells. J. Membr. Biol. 154, 205–216.

Hu, H., Sachs, F., 1997. Stretch-activated ion channels in the heart. J. Mol. Cell. Cardiol. 29, 1511–1523.

Isenberg, G., Klockner, U., 1982. Calcium tolerant ventricular myocytes prepared by preincubation in a "KB medium". Pflugers. Arch. 395, 6–18.

Kalifa, J., Jalife, J., Zaitsev, A.V., Bagwe, S., Warren, M., Moreno, J., Berenfeld, O., Nattel, S., 2003. Intra-atrial pressure increases rate and organization of waves emanating from the superior pulmonary veins during atrial fibrillation. Circulation 108, 668–671.

Kamkin, A., Kiseleva, I., Isenberg, G., 2000. Stretch-activated currents in ventricular myocytes: amplitude and arrhythmogenic effects increase with hypertrophy. Cardiovasc. Res. 48, 409–420.

Kamkin, A., Kiseleva, I., Isenberg, G., 2003a. Ion selectivity of stretch-activated cation currents in mouse ventricular myocytes. Pflugers. Arch. 446, 220–231.

Kamkin, A., Kiseleva, I., Wagner, K.D., Bohm, J., Theres, H., Gunther, J., Scholz, H., 2003b. Characterization of stretch-activated ion currents in isolated atrial myocytes from human hearts. Pflugers. Arch. 446, 339–346.

Kim, D., 1993. Novel cation-selective mechanosensitive ion channel in the atrial cell membrane. Circ. Res. 72, 225–231.

Knackstedt, C., Visser, L., Plisiene, J., Zarse, M., Waldmann, M., Mischke, K., Koch, K.C., Hoffmann, R., Franke, A., Hanrath, P., Schauerte, P., 2003. Dilatation of the pulmonary veins in atrial fibrillation: a transesophageal echocardiographic evaluation. Pacing. Clin. Electrophysiol. 26, 1371–1378.

Leem, C.H., Kim, W.T., Ha, J.M., Lee, Y.J., Seong, H.C., Choe, H., Jang, Y.J., Youm, J.B., Earm, Y.E., 2006. Simulation of Ca^{2+}-activated Cl^{-} current of cardiomyocytes in rabbit pulmonary vein: implications of subsarcolemmal Ca^{2+} dynamics. Philos. Transact. A Math. Phys. Eng. Sci. 364, 1223–1243.

Levy, S., 1998. Epidemiology and classification of atrial fibrillation. J. Cardiovasc. Electrophysiol. 9, S78–S82.

Lin, W.S., Prakash, V.S., Tai, C.T., Hsieh, M.H., Tsai, C.F., Yu, W.C., Lin, Y.K., Ding, Y.A., Chang, M.S., Chen, S.A., 2000. Pulmonary vein morphology in patients with paroxysmal atrial fibrillation initiated by ectopic beats originating from the pulmonary veins: implications for catheter ablation. Circulation 101, 1274–1281.

Matsuda, N., Hagiwara, N., Shoda, M., Kasanuki, H., Hosoda, S., 1996. Enhancement of the L-type Ca^{2+} current by mechanical stimulation in single rabbit cardiac myocytes. Circ. Res. 78, 650–659.

Moe, G.K., Abildskov, J.A., 1959. Atrial fibrillation as a self-sustaining arrhythmia independent of focal discharge. Am. Heart. J. 58, 59–70.

Morillo, C.A., Klein, G.J., Jones, D.L., Guiraudon, C.M., 1995. Chronic rapid atrial pacing. Structural, functional, and electrophysiological characteristics of a new model of sustained atrial fibrillation. Circulation 91, 1588–1595.

Nam, G.B., Choi, K.J., Leem, C.H., Kim, Y.H., 2000. The characteristics of spontaneous action potentials if myocytes in rabbit pulmonary vein: implication ininitiation mechanism of focal atrial fibrillation. PACE 23, 604:206P.

Nathan, H., Eliakim, M., 1966. The junction between the left atrium and the pulmonary veins. An anatomic study of human hearts. Circulation 34, 412–422.

Nattel, S., 2002. New ideas about atrial fibrillation 50 years on. Nature 415, 219–226.

Nattel, S., Li, D., Yue, L., 2000. Basic mechanisms of atrial fibrillation—very new insights into very old ideas. Annu. Rev. Physiol. 62, 51–77.

Ogura, T., Matsuda, H., Imanishi, S., Shibamoto, T., 2002. Sarcolemmal hydraulic conductivity of guinea-pig and rat ventricular myocytes. Cardiovasc. Res. 54, 590–600.

Psaty, B.M., Manolio, T.A., Kuller, L.H., Kronmal, R.A., Cushman, M., Fried, L.P., White, R., Furberg, C.D., Rautaharju, P.M., 1997. Incidence of and risk factors for atrial fibrillation in older adults. Circulation 96, 2455–2461.

Ravelli, F., Allessie, M., 1997. Effects of atrial dilatation on refractory period and vulnerability to atrial fibrillation in the isolated Langendorff-perfused rabbit heart. Circulation 96, 1686–1695.

Rees, S.A., Vandenberg, J.I., Wright, A.R., Yoshida, A., Powell, T., 1995. Cell swelling has differential effects on the rapid and slow components of delayed rectifier potassium current in guinea pig cardiac myocytes. J. Gen. Physiol. 106, 1151–1170.

Ruknudin, A., Sachs, F., Bustamante, J.O., 1993. Stretch-activated ion channels in tissue-cultured chick heart. Am. J. Physiol. 264, H960–H972.

Ruskin, J.N., Singh, J.P., 2004. Atrial fibrillation endpoints: hospitalization. Heart Rhythm 1, B31-4, discussion B34-5.

Sadoshima, J., Takahashi, T., Jahn, L., Izumo, S., 1992. Roles of mechano-sensitive ion channels, cytoskeleton, and contractile activity in stretch-induced immediate-early gene expression and hypertrophy of cardiac myocytes. Proc. Natl. Acad. Sci. USA 89, 9905–9909.

Sasaki, N., Mitsuiye, T., Noma, A., 1992. Effects of mechanical stretch on membrane currents of single ventricular myocytes of guinea-pig heart. Jpn. J. Physiol. 42, 957–970.

Sasaki, N., Mitsuiye, T., Wang, Z., Noma, A., 1994. Increase of the delayed rectifier K^+ and Na^+–K^+ pump currents by hypotonic solutions in guinea pig cardiac myocytes. Circ. Res. 75, 887–895.

Schotten, U., Neuberger, H.R., Allessie, M.A., 2003. The role of atrial dilatation in the domestication of atrial fibrillation. Prog. Biophys. Mol. Biol. 82, 151–162.

Seol, C.A., Kim, J., Kim, W.T., Ha, J.M., Choe, H., Jang, Y.J., Shim, E.B., Youm, J.B., Earm, Y.E., Leem, C.H., 2008. Simulation of spontaneous action potentials of cardiomyocytes in pulmonary veins of rabbits. Prog. Biophys. Mol. Biol. 96, 132–151.

Sideris, D.A., Toumanidis, S.T., Thodorakis, M., Kostopoulos, K., Tselepatiotis, E., Langoura, C., Stringli, T., Moulopoulos, S.D., 1994. Some observations on the mechanism of pressure related atrial fibrillation. Eur. Heart. J. 15, 1585–1589.

Sokabe, M., Hasegawa, N., Yamamori, K., 1993. Blockers and activators for stretch-activated ion channels of chick skeletal muscle. Ann. NY Acad. Sci. 707, 417–420.

Sorota, S., 1992. Swelling-induced chloride-sensitive current in canine atrial cells revealed by whole-cell patch-clamp method. Circ. Res. 70, 679–687.

Sorota, S., 1994. Pharmacologic properties of the swelling-induced chloride current of dog atrial myocytes. J. Cardiovasc. Electrophysiol. 5, 1006–1016.

Sra, J., Dhala, A., Blanck, Z., Deshpande, S., Cooley, R., Akhtar, M., 2000. Atrial fibrillation: epidemiology, mechanisms, and management. Curr. Prob. Cardiol. 25, 405–524.

Stones, R., Gilbert, S., Benoist, D., White, Ed., 2008. Inhomogeneity in the response to mechanical stimulation: Cardiac muscle function and gene expression. Prog. Biophys. Mol. Biol. 97, 268–281.

Suleymanian, M.A., Baumgarten, C.M., 1996. Osmotic gradient-induced water permeation across the sarcolemma of rabbit ventricular myocytes. J. Gen. Physiol. 107, 503–514.

Tasaki, H., 1969. Electrophysiological study of the striated muscle cells of the extrapulmonary vein of the guinea-pig. Jpn. Circ. J. 33, 1087–1098.

Tsao, H.M., Wu, M.H., Yu, W.C., Tai, C.T., Lin, Y.K., Hsieh, M.H., Ding, Y.A., Chang, M.S., Chen, S.A., 2001. Role of right middle pulmonary vein in patients with paroxysmal atrial fibrillation. J. Cardiovasc. Electrophysiol. 12, 1353–1357.

Tseng, G.N., 1992. Cell swelling increases membrane conductance of canine cardiac cells: evidence for a volume-sensitive Cl channel. Am. J. Physiol. 262, C1056–C1068.

Van Wagoner, D.R., 1993. Mechanosensitive gating of atrial ATP-sensitive potassium channels. Circ. Res. 72, 973–983.

Vandenberg, J.I., Yoshida, A., Kirk, K., Powell, T., 1994. Swelling-activated and isoprenaline-activated chloride currents in guinea pig cardiac myocytes have distinct electrophysiology and pharmacology. J. Gen. Physiol. 104, 997–1017.

Vandenberg, J.I., Rees, S.A., Wright, A.R., Powell, T., 1996. Cell swelling and ion transport pathways in cardiac myocytes. Cardiovasc. Res. 32, 85–97.

Vasan, R.S., Larson, M.G., Levy, D., Evans, J.C., Benjamin, E.J., 1997. Distribution and categorization of echocardiographic measurements in relation to reference limits: the Framingham Heart Study: formulation of a height- and sex-specific classification and its prospective validation. Circulation 96, 1863–1873.

Vaziri, S.M., Larson, M.G., Benjamin, E.J., Levy, D., 1994. Echocardiographic predictors of nonrheumatic atrial fibrillation. The Framingham Heart Study. Circulation 89, 724–730.

Wijffels, M.C., Kirchhof, C.J., Dorland, R., Allessie, M.A., 1995. Atrial fibrillation begets atrial fibrillation. A study in awake chronically instrumented goats. Circulation 92, 1954–1968.

Wolf, P.A., Abbott, R.D., Kannel, W.B., 1991. Atrial fibrillation as an independent risk factor for stroke: the Framingham Study. Stroke 22, 983–988.

Yamane, T., Shah, D.C., Jais, P., Hocini, M., Peng, J.T., Deisenhofer, I., Clementy, J., Haissaguerre, M., 2002. Dilatation as a marker of pulmonary veins initiating atrial fibrillation. J. Interv. Card. Electrophysiol. 6, 245–249.

Youm, J.B., Ho, W.K., Earm, Y.E., 2000. Permeability characteristics of monovalent cations in atrial myocytes of the rat heart. Exp. Physiol. 85, 143–150.

Zeng, T., Bett, G.C., Sachs, F., 2000. Stretch-activated whole cell currents in adult rat cardiac myocytes. Am. J. Physiol. Heart. Circ. Physiol. 278, H548–H557.

Zhang, Y.H., Youm, J.B., Sung, H.K., Lee, S.H., Ryu, S.Y., Ho, W.K., Earm, Y.E., 2000. Stretch-activated and background non-selective cation channels in rat atrial myocytes. J. Physiol. 523 (Pt. 3), 607–619.